Mon. Not. R. astr. Soc. (1991) **251**, *Short Communication*, 41P–45P

Superclusters are warm, not hot: the predicted flux distribution of soft X-rays

A. A. Klypin[1] and R. E. Kates[2]
[1]*Lebedev Physical Institute, 117810 Moscow, USSR*
[2]*Max-Planck-Institut für Astrophysik, W-8046 Garching, Germany*

Accepted 1991 May 23. Received 1991 March 27; in original form 1990 November 30

SUMMARY

We present arguments showing that gas present in superclusters should have a characteristic temperature of approximately 10^6 K. In the most popular models of large-scale structure formation, including hot and cold dark matter, peculiar velocities of matter relative to the background are ≈ 1000 km s^{-1}. This would imply temperatures exceeding 10^7 K. However, most of the peculiar motions can be attributed to large-scale, coherent velocities. Moreover, gas inside superclusters which is not concentrated in groups or clusters will cool adiabatically with the Hubble expansion. A temperature of 10^6 K implies that radiation from gas in superclusters should not be seen in X-rays of energy > 500 eV. The most favourable range for observing this radiation is about 100–300 eV. We present the results of numerical simulations of the evolution of large-scale structure in a cold dark matter (CDM) scenario *including the thermal history of the baryonic component.* These simulations provide estimates of the flux, together with examples of patterns as they would appear in the data. Soft X-rays emitted from hot gas in known superclusters may be detectable at the limits of sensitivity of *ROSAT* by averaging counts over a sufficiently large region.

1 INTRODUCTION

Efforts to search for X-ray emission from gas inside superclusters give only upper limits for the flux (Ulmer & Cruddace 1981; Ku *et al.* 1983; Persic *et al.* 1990). However, all of these observations were made in an energy band above 1 keV, which is appropriate for a gas temperature $T_{\rm gas} \approx 10^7$ K. Indeed, it should come as no great surprise that X-ray emission from superclusters was not detected in this band: as we shall shortly see, the most likely estimate for $T_{\rm gas}$ is only about 10^6 K.

Future X-ray satellites will offer increased sensitivity in the energy window below 500 eV. This suggests that it may be possible to detect diffuse emission from superclusters. Thus, it is important to understand the characteristics of the signal, including the expected flux and spatial distribution. Comparison of the measurements with theory could provide a new test of different models for large-scale structure and galaxy formation. It could also provide information about the composition of the intergalactic medium in superclusters.

The hot dark matter (HDM) model of galaxy formation predicts that the temperature in superclusters (which correspond to pancakes) should reach a level of $T_{\rm gas} \approx 10^7$ K. However, HDM seems to be in conflict with a variety of measurements and observations. In the CDM model peculiar motions of *dark matter* relative to the background are about 500–1000 km s^{-1}, which naively would imply a temperature $T_{\rm gas} \approx 10^7$ K or more. However, much of the power in peculiar velocities can be attributed to flows which are coherent on scales even larger than a supercluster. Typical internal velocities of galaxies on scales of 1 Mpc were estimated by Kates, Kotok & Klypin (1991; Paper I) to be about 350 km s^{-1} for a model with the biasing parameter $b = 1.7$. This roughly corresponds to a temperature $T_{\rm gas} \approx 3 \times 10^6$ K. Recent evidence suggests that the power in the CDM model may be deficient at scales of ≈ 100 Mpc. An increase in power at these scales could have some effect on $T_{\rm gas}$ in the case of a 'Great Wall' or 'Great Attractor', and thus results obtained using the *standard* CDM model might need modification if one happens to be dealing with such objects.

Observations also seem to lend indirect support to the hypothesis that $T_{\rm gas} \approx 10^6$ K. Davis & Peebles (1983) found that relative peculiar motions in pairs of galaxies at a distance of 1 Mpc are about 340 km s^{-1}. Some light is also shed on the question by an analysis of the velocity dispersion of galaxies in the peripheral regions (distances greater than 2 Mpc) of rich clusters. For example, the results of Rood, Page & Kintner (1972), Chincarini & Rood (1976), and Thompson & Gregory (1978) are consistent with a decrease of the velocity dispersion in the outer regions of the Coma

Cluster to ≈ 400 km s^{-1}, and similar results were obtained for A194 by Chincarini & Rood (1977). The peculiar Virgocentric velocity of the Local Group is in the range 150–350 km s^{-1} (Dressler 1984; Dressler *et al.* 1987).

Further indirect information concerning the typical small-scale 'noise' velocity can be derived from fits of distance indicator data to Great Attractor models or other models of the large-scale velocity field. The 'noise' reported by Dressler *et al.* (1987) corresponds to a three-dimensional velocity dispersion of ≈ 700 km s^{-1}. More recently, using a new calibration (Weigelt & Kates 1990) of the D_n–σ relation, Weigelt & Kates (1991a) estimated a value of ≈ 600 km s^{-1} from the residuals of a fit to a model allowing for both bulk streaming and an attractor. However, since the residuals still include power on scales ranging from a few to about 50 Mpc, this estimate should be interpreted as an upper bound, i.e., some large fraction of this power should presumably be attributed to coherent motions of either the entire supercluster or large fragments of it. Indeed, a higher order fit reduces the residuals to a value corresponding to less than ≈ 400 km s^{-1} (Weigelt & Kates 1991b).

The peculiar velocities estimated by both theoretical and observational arguments would roughly correspond to $T_{\rm gas} \approx 10^6$ K – if one were to assume that the velocity dispersion of gas particles equals that of galaxies. In any case, to relate these estimates properly requires a physical model. In particular, an accurate estimate requires direct simulation of the thermal history of the gas in the context of a scenario for the formation of large-scale structure.

In this paper, we focus our attention on the possibility of detecting the soft X-ray flux that would be seen by an observer in an energy band appropriate for *ROSAT*. The results are somewhat more favourable than what might have been expected from order-of-magnitude considerations. If we bin pixels in cells of about $(30 \times \text{arcmin})^2$, detailed computation shows that about 5 per cent of the cells have fluxes of about 1/10 of a level which could be detected by *ROSAT* in a reasonable observing time. However, since the high-flux cells are correlated along known superclusters, *there is some hope of boosting the number of counts to about the level of the noise.*

2 MODEL

The details of our model were explained in Paper I, and thus for brevity we summarize here only the main considerations of this paper: we simulate the kinematics of dark matter and the thermal history of baryons. However, the dynamic range (ratio of largest to smallest resolved scale) in this problem is intrinsically high and therefore requires very good resolution. This resolution cannot be achieved at present if hydrodynamic effects are simulated directly. For this reason, the baryonic material is treated as if the baryon trajectories were the same as those of the dark matter. (This means of course that the acceleration due to pressure gradients is neglected.) Thus, we assume that the local gas density is proportional to the local density of dark matter, i.e. $\rho_{\rm gas} \equiv \rho \Omega_{\rm b}$, where $\Omega_{\rm b} = 0.1$ is the background fraction of baryons. This assumption is definitely valid before the formation of the first shocks, when the medium is still cold and fluctuations are small (in our model we put $T_{\rm gas} = 0$ at $z_{\rm start} = 25$). As perturbations grow, eventually the first objects start to collapse, producing caustics in the dark matter and shocks in the gas. As simple pancake models show (Shapiro & Struck-Marcell 1985), shocks occur close to caustics. At a shock, the temperature acquired by gas particles with velocity $\boldsymbol{v}$ is given by

$$kT = \mu_{\rm M} m_{\rm H} (\boldsymbol{v} - \boldsymbol{U})^2/3, \qquad (1)$$

where $\boldsymbol{U}$ is the local velocity, $m_{\rm H}$ is the mass of hydrogen, and $\mu_{\rm M}$ is the molecular weight per particle. This was the estimate used in our numerical model. It is insensitive to small errors in the position of the shock, because the local velocity is a smoothly varying function of the spatial coordinates.

From this moment on, the kinematical behaviour of gas differs strongly from that of the dark matter within clumps. Gas stops at the shock front, whereas dark matter particles fall freely into the clump and oscillate between turning points of their motion in the clump potential well. Nevertheless, dark matter spends a large fraction of its time at about the same radius as the gas, because they originally had the same kinetic energy. Indeed, results of a 1D-pancake test presented in Paper I show good agreement of our model with hydrodynamical simulations (20 per cent of cooled gas, position of cooling front and shock wave). There are two situations in which our approach would be expected to fail: first, when gas starts to cool efficiently – this happens inside dense regions and/or if the temperature becomes too low ($T < 2 \times 10^5$ K). Secondly, when gas undergoes secondary shocking in our present model, this means collapse to objects with masses larger than a galactic mass. (Note that our smallest resolved scale corresponds to a mass of $\approx 10^{10}\, M_\odot$.) Thus, the internal regions of galaxies and clusters are not treated properly, but our method gives a reasonable approximation for the behaviour of gas which moved from voids and was trapped in the potential wells of superclusters and filaments. The thermal history of this material is of primary interest for our present considerations.

Positions of shocks are found in the numerical model as follows. Particles for which the Jacobian determinant of the transformation from Lagrangian to Eulerian coordinates is negative are classified as shocked, as well as particles passing through a region containing previously shocked particles. When a particle crosses a shock and is assigned a temperature, we start to integrate the energy equation along the trajectory of the particle:

$$\frac{dT}{dt} = (\gamma - 1)\left[\frac{T}{n_{\rm H}}\frac{dn_{\rm H}}{dt} - \frac{\mu_{\rm M}}{\mu_{\rm H}}\frac{1}{k n_{\rm H}}(\Lambda_{\rm rad} + \Lambda_{\rm Comp})\right], \qquad (2)$$

where $n_{\rm H}$ is the number density of hydrogen atoms, $\mu_{\rm H}$ is the molecular weight by hydrogen atom, $\rho_{\rm gas} \equiv \rho \Omega_{\rm b} = n_{\rm H} \mu_{\rm M} m_{\rm H}$. Here, $\Lambda_{\rm rad}$ represents radiative losses in the hot plasma, and $\Lambda_{\rm Comp}$ is the cooling rate due to Compton scattering.

In computing $\Lambda_{\rm rad}$, we suppose that the intergalactic gas has *primordial abundances:* this model is certainly reasonable during the early stages of our simulation for $z > 5$. Later, the intergalactic medium could have been enriched. This definitely occurred for gas in rich clusters of galaxies, but the degree of enrichment of gas in superclusters is not known. However, we know that the metallicity of the intracluster medium drops off at increasing radius within clusters and does not exceed one-tenth of solar abundances beyond a radius of about 0.5 Mpc (Ponman *et al.* 1990),

which could indicate that gas in superclusters is not substantially enriched by heavy elements. Moreover, physical mechanisms of enrichment of gas in rich clusters – stripping of gas when a galaxy moves through a medium with high pressure and galaxy collisions – are much less efficient in superclusters because the gas density, the number density of galaxies, and the peculiar velocities are lower. In any case, X-ray observations could give important clues to the composition of the intergalactic medium in superclusters.

Now, when material cools below 10^4 K, stars will form, producing luminous matter. By assigning the label 'cooled' to the particles with $T < 10^4$ K, we have a measure for the amount of visible matter. However, we know that the efficiency for the conversion of gas to stars is low. To simulate this effect, we 'reheat' to the temperature $T_{\rm reheat} = 5 \times 10^5$ K those particles which have cooled to below 10^4 K with a probability of 85 per cent and assign to the remaining 15 per cent the label 'cooled'. Some of the reheated particles later will attain high temperatures, provided they enter collapsing regions of high density. Other particles can simply cool again and turn into 'visible' matter. The probabilities of the reheating process (85/15 per cent) were fitted to obtain a reasonable fraction of cooled gas: 1/3 of all the gas in collapsed objects (mainly superclusters) was still 'hot' at $z = 0$. As long as the probability to become 'cold' is small, the results are not very sensitive to the particular choice of parameters. We tried a 90/10 per cent combination with essentially the same results.

It should be emphasized that *some* mechanism preventing conversion of the gas to luminous matter is *inevitable* for the CDM model: otherwise, all the gas would simply collapse, forming stars and ending up in globular clusters long before the formation of large objects.

The initial conditions for our simulations correspond to a 'standard' CDM spectrum (Bardeen *et al.* 1986). The normalization can be expressed in terms of a 'biasing parameter' b, which, as usual, is defined as the ratio of $\delta M/M$ fluctuations in dark matter to $\delta N/N$ in galaxy counts for a randomly placed sphere of radius 16 Mpc ($h = 0.5$). For our model, $b = 1.7$, which corresponds to a 3D rms velocity of 760 km s^{-1} for dark matter particles with respect to the rest frame of the microwave background, as extrapolated by linear theory to $z = 0$.

The Zel'dovich approximation is used until $z = 25$. After this, using a particle-mesh (PM) code, we evolve the usual Euler–Poisson system describing the evolution of self-gravitating, collisionless matter. The computations were performed in a box of size 100 Mpc ($H_0 = 50$ km s^{-1} Mpc^{-1}) with periodic boundary conditions. The amplitude of the initial fluctuations was adjusted to account for the finite size of the box. Accordingly, the 3D rms extrapolated velocity of the dark matter was not 760 km s^{-1}, but 695 km s^{-1}, the remaining power being attributed to coherent motion of the box as a whole with respect to the rest frame of the microwave background.

We emphasize that the calculation places stringent requirements on the resolution: a large computational box of at least 100 Mpc is necessary for a proper simulation of supercluster formation, while accurate estimates of X-ray emission require a proper treatment of small-scale effects such as heating and cooling. Our model comprises 128^3 particles on a 256^3 grid. The cell size is thus 0.39 Mpc, and the mass of one particle is $3.3 \times 10^{10}\ M_\odot$. Although ignoring hydrodynamic effects leads to certain inaccuracies as discussed above, it permits one to achieve very good resolution, without which this problem cannot be treated with any degree of reliability.

For problems requiring an accurate description of gas dynamics such as the formation and evolution of clusters, there does not seem to be any alternative at present to direct hydrodynamical simulations such as those of Cen *et al.* (1990) and Loeb & Ostriker (1991). As it turns out, so some extent their results lend support to our approach: they also find that the baryonic and dark matter distributions look remarkably similar (see fig. 3 of Cen *et al.*) and that most of the gas in regions with density $\rho > 10\langle\rho\rangle$ has a temperature between 10^6 and 10^7 K. Unfortunately, their resolution does not yet permit them to follow large and small scales in the same model, which is crucial for many aspects of the present problem.

3 RESULTS

To get an idea of the structures in the model, we show a slice of thickness 4 Mpc in Fig. 1. Cooled particles (Fig. 1a) represent luminous matter. Although not all cooled particles are associated with galaxies, they trace the distribution of galaxies more closely than dark matter. The concentration of particles in the upper left corner corresponds to one of the two large clusters of galaxies which formed in the simulation. Fig. 1(b) shows the distribution of warm gas in this slice. Warm gas traces the more massive filaments visible in 1(a). (Here the term 'filaments' refers either to true filaments or to walls, since in a thin slice it is difficult to distinguish between them.) These filaments are no longer evident if we consider hot gas with temperature $T > 10^7$ K (Fig. 1c), where mainly clusters and large groups are seen.

Efficient emission of soft X-rays requires both the proper temperature and an adequate gas density. Fig. 1(d) shows warm ($5 \times 10^5 < T < 5 \times 10^6$ K) particles in regions where the hydrogen number density exceeds 2×10^{-6} cm^{-3}. Here, the distribution is much clumpier, but still the filamentary structures are seen.

In order to model an experimental situation, we simulated the angular distribution on the sky of the X-ray flux in the energy range 150–300 eV, as shown in Fig. 2. (This is an appropriate energy window for *ROSAT*.) We consider a cone of diameter 60° with vertex in the middle of one face of a cube consisting of 2^3 simulation boxes. The flux seen by this observer is computed using the known distribution of temperature T and hydrogen density $n_{\rm H}$ from the simulation. Contributions from particles with $5 \times 10^5 < T < 10^7$ K were included. Sources closer than 10 Mpc from the observer were excluded.

4 DISCUSSION

For comparison with the sensitivity of *ROSAT* and future experiments, it is useful to obtain a fiducial estimate of the flux in the window 150–300 eV. Below this range the galaxy is not transparent to X-rays, whereas above this range the contribution of gas in superclusters is low. Our simulations yield a typical gas density in superclusters of $n_{\rm H} \approx 2 \times 10^{-6}$

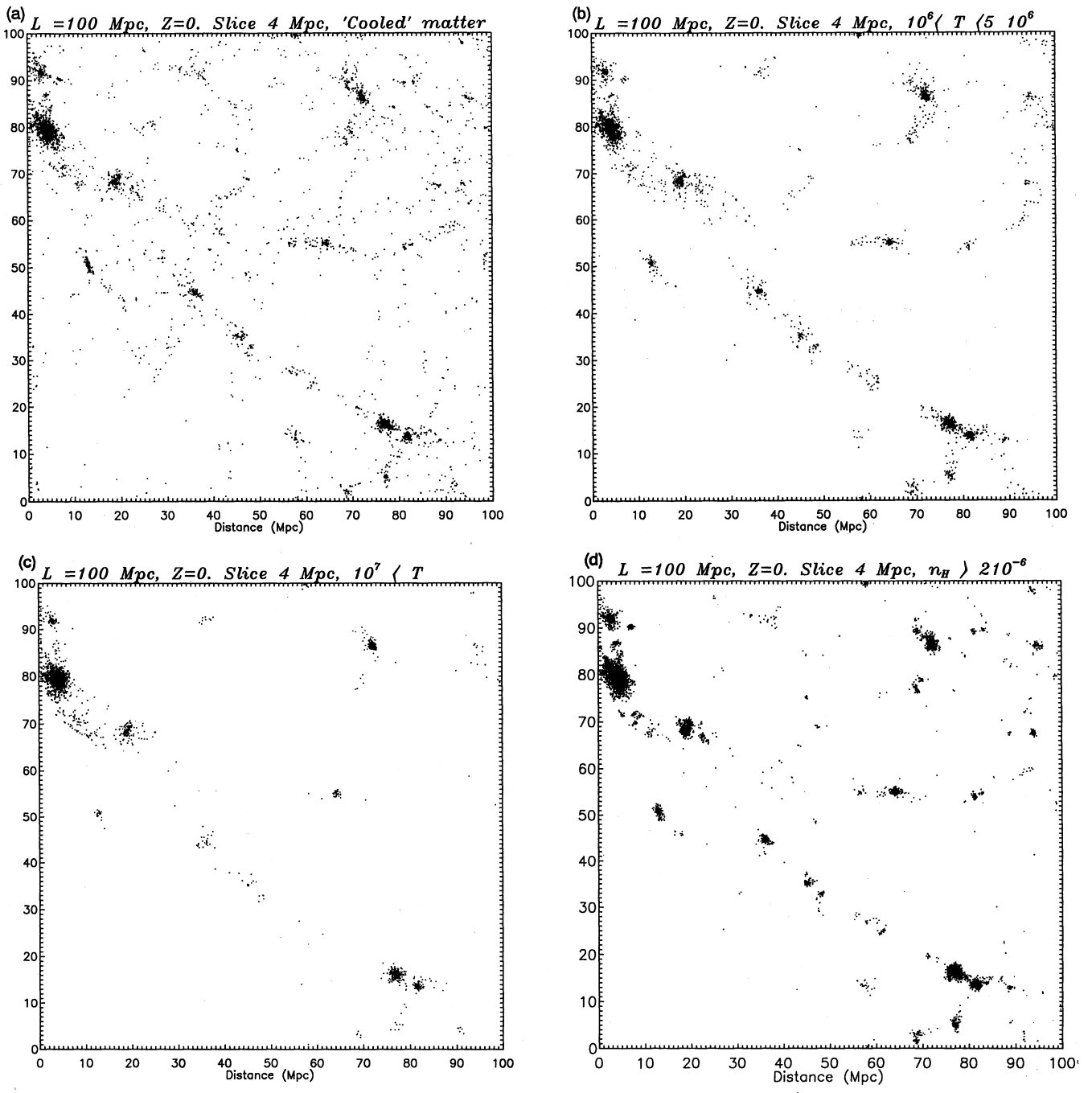

Figure 1. Distribution of different components of matter in a slice of thickness 4 Mpc. (a) Cooled particles (1/12 of particles shown). (b) Particles with temperature $10^6 < T < 5 \times 10^6$. (c) Particles with $T > 10^7$ K. (d) Particles with hydrogen number density $n_H > 2 \times 10^{-6}$ cm^{-3}.

cm^{-3}. [A similar estimate for n_H can be obtained from the 'King' formula for the density of gas in clusters $n_H(r) = n_0[1 + (r/r_c)^2]^{-3/2}$, with $n_0 = 10^{-3}$ cm^{-3}, $r_c = 0.5$ Mpc, and $r = 5$ Mpc.] The emissivity can be estimated taking into account free–free and free–bound emission. Gas with temperature between 5×10^5 and 10^7 K contributes about equally at the level $\Lambda/n_H^2 = 2 \times 10^{-24}$ erg cm^{-3} s^{-1} *to this energy window.* Consider a supercluster located at a distance of 100 Mpc. If the thickness is 1 Mpc, we should look at a cell of area (30 × arcmin)^2, corresponding to two cells across the width. (This implies that we will average counts over many pixels of the detector.) With these parameters, the flux from a volume element of size (2 Mpc)^3 is therefore $\approx 5 \times 10^{-15}$ erg cm^{-2} s^{-1}. For the *ROSAT* PSPC instrument, this fiducial flux leads to about 0.2 counts in a cell in a time 1000 s. This compares to a noise level (fluctuations from the galactic background, etc.) of 30 counts in the same cell and time. (The total background is much larger.) In order for the fiducial flux to be detectable, an improvement of about 150 in the effective detector area would be necessary.

Fig. 2(a) shows that the predicted flux density on the sky exceeds the fiducial level by a factor of about 15 for 5 per cent of the cells. For these high-flux cells, the expected number of counts is still about a factor of 10 below the noise

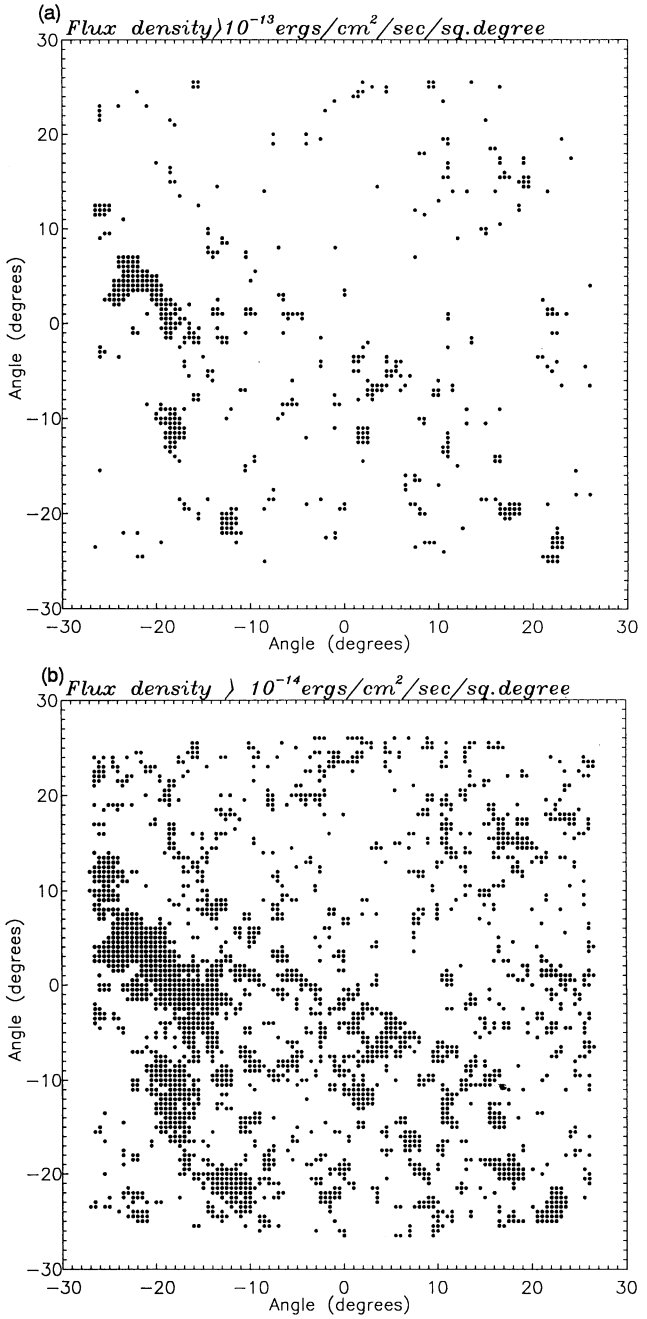

Figure 2. Simulated angular distribution of X-ray flux density on the sky [region of size $(30°)^2$ in the energy window 150–300 eV, binned in cells of size $(30\ \text{arcmin})^2$]. (a) Cells with flux exceeding 10^{-13} erg s^{-1} cm^{-2} deg^{-2} (about 5 per cent of total area). (b) Cells with flux exceeding 10^{-14} erg s^{-1} cm^{-2} deg^{-2} (about 17 per cent of total area). A flux of 10^{-13} erg s^{-1} cm^{-2} deg^{-2} corresponds to about 3 counts in 1000 s of observation for the *ROSAT* PSPC detector in a 30-arcmin cell. The expected background fluctuation level in a cell of this width would be 30 counts.

level. Note, however, that they have the appearance of a band extending across the figure, and there are large regions of at least 10° on a side containing only a few high-flux cells . (A qualitatively similar pattern was found in a different projection.)

An additional improvement by a factor ≈ 10–20 might be achievable if the most favourable (high-flux) cells were located along some *known* supercluster. Therefore, our simulation predicts that it is not unreasonable to hope that soft X-rays due to hot gas in superclusters may be detectable at the limits of sensitivity of *ROSAT*.

Our numerical estimates of the X-ray fluxes should depend on the particular choice of model parameters (biasing parameter b, parameters of the 'reheating' mechanism). But it seems that the chemical abundance has the strongest effect: the cooling rate with solar abundances is an order of magnitude higher than with primordial composition. Nevertheless, our results show that there are rather firm arguments in favour of searching for X-ray emission from superclusters, not in the high-energy band, but at low energies (100–300 eV) and that there is some hope of observing superclusters in X-rays in the very near future.

REFERENCES

Bardeen, J. M., Bond, J. R., Kaiser, N. & Szalay, A. S., 1986. *Astrophys. J.*, **304,** 15.

Cen, R. Y., Jameson, A., Liu, F. & Ostriker, J. P., 1990. *Astrophys. J.*, **362,** L41.

Chincarini, G. & Rood, H., 1976. *Astrophys. J.*, **206,** 30.

Chincarini, G. & Rood, H., 1977. *Astrophys. J.*, **214,** 351.

Davis, M. & Peebles, P., 1983. *Astrophys. J.*, **267,** 465.

Dressler, A., 1984. *Astrophys. J.*, **281,** 512.

Dressler, A., Lynden-Bell, D., Burstein, D., Davies, R., Faber, S., Terlevich, R. & Wegner, G., 1987. *Astrophys. J.*, **313,** 42.

Kates, R., Kotok, N. & Klypin, A., 1991. *Astr. Astrophys.*, in press (Paper I).

Ku, W., Abramopoulos, F., Nulsen, P., Fabian, A., Stewart, G., Chincarini, G. & Tarenghi, M., 1983. *Mon. Not. R. astr. Soc.*, **203,** 253.

Loeb, A. & Ostriker, J., 1991. Preprint.

Persic, M., Jahoda, K., Rephaeli, Y., Boldt, E., Marshall, F. E., Mushotzky, R. F. & Rawley, G., 1990. *Astrophys. J.*, **364,** 1.

Ponman, T., Bertram, D., Church, M., Eyles, C., Watt, M., Skinner, G. & Willmore, A., 1990. *Nature,* **347,** 450.

Rood, H., Page, T. & Kintner, E., 1972. *Astrophys. J.*, **175,** 627.

Shapiro, P. & Struck-Marcell, C., 1985. *Astrophys. J. Suppl.*, **57,** 205.

Thompson, L. & Gregory, S., 1978. *Astrophys. J.*, **220,** 809.

Ulmer, M. & Cruddace, R., 1981. *Astrophys. J. Lett.*, **246,** L99.

Weigelt, U. & Kates, R., 1990. *Astr. Astrophys.*, in press.

Weigelt, U. & Kates, R., 1991a. *Mon. Not. R. astr. Soc.*, submitted.

Weigelt, U. & Kates, R., 1991b. Preprint.